# Synthesis of passive interconnections in mass chains achieving a scale-free performance

Yamamoto, Kaoru
Faculty of Information Science and Electrical Engineering, Kyushu University



出版情報：Proceedings of the Institution of Mechanical Engineers, Part I: Journal of Systems and Control Engineering. 235 (9), pp.1709-1717, 2021-10-01. SAGE Publications
バージョン：

# Synthesis of passive interconnections in mass chains achieving a scale-free performance

Journal Title
XX(X):1–8

DOI: 10.1177/ToBeAssigned
www.sagepub.com/
SAGE

**Kaoru Yamamoto**[1]

**Abstract**

This paper is concerned with the synthesis problem of passive mechanical admittances that connect masses in a chain. The mass chain is excited at one boundary point, and the admittances are designed to suppress the disturbance independent of the length of the chain. The scalar transfer functions from the disturbance to a given intermass displacement are studied. The disturbance rejection performance is optimised over a class of arbitrary positive real mechanical admittances. The resulting admittance is synthesised mechanically using springs, dampers, and inerters only.

**Keywords**

Mass chain, network synthesis, large-scale network

## Introduction

In recent years, it has become of great interest to consider the systems that involve very large numbers of locally interconnected subsystems. In such applications, the number of subsystems is often subject to change and it is desirable to ensure the ability to control a system behaviour independent of the size of the systems. We call such ability as a *scale-free* property. For a system that possesses a scale-free property, any design remains valid even if the number of subsystems changes. A mass chain is an ideal model to analyse such a property. The problem of passive control of a mass chain arises in the design of a variety of mechanical systems including multi-storey buildings subjected to disturbances such as an earthquake disturbance or wind,[1,2] and dynamic vibration absorbers.[3,4] Instead of the conventional interconnection configuration consisting of springs and dampers only, we consider passive interconnections of the most general type, as shown in Fig. 1, which may require the use of inerters.[5] In recent years, mass chain systems including inerters have been intensively studied[6–8] because of its potential to give us much greater flexibility in control design. For example, it is possible to assign any arbitrary given set of positive distinct numbers as the natural frequencies of the mass chain of Fig. 1 where each interconnection is a parallel combination of a spring and an inerter.[9,10]

This general mass chain model is also suitable to analyse vehicle platoons, where the inter-vehicle spacing regulation policy is modelled as a virtual impedance. In this application, there is a phenomenon called string instability where the disturbance entered in the platoon propagates along the string causing instability as a whole despite each car is stable.[11–13] Network incoherence phenomena are also reported in the literature.[14] Nonetheless, it appears that average or local performance measures can sometimes be guaranteed in a scale-free manner.[15–18]

In particular, the author has shown[16,19] that the $H^\infty$-norm of the transfer function from the disturbance at one end to a given intermass displacement in the mass chain is uniformly bounded with respect to $N$ for certain choices of interconnection admittances. The conditions have been given with respect to a dimensionless parameter $h$ depending on the admittance and the mass. A graphical means to design suitable interconnection admittances has been proposed[16,19–21] so that the supremum of the $H^\infty$-norm over $N$ is no greater than a prescribed value. This can be thought of as a scale-free $H^\infty$ control design for an infinite family of plants in which the interconnection admittance is the controller. However, one drawback of this graphical method is that one needs to manually shape the Nyquist diagram of $h(s)$. The procedure typically requires to first fix the interconnection network configuration and then tune the parameters of the passive components. Therefore, it is difficult to search over a broad class of interconnection admittances.

In the present paper we aim to seek a (sub)optimal interconnection network configuration that minimises the supremum of the $H^\infty$-norm over $N$ in the mass chain of Fig. 1. A class of *arbitrary* positive real mechanical admittances of fixed degree is searched over for the optimisation. The resulting admittance is then realised as a network with springs, inerters, and dampers only.[5] This is a mechanical analogue of a key result from electrical network synthesis,[22] which is summarised in the next section. To illustrate the concept of the proposed method, we consider degree-3 positive real admittances since the

[1]Kyushu University, Japan

**Corresponding author:**
Kaoru Yamamoto, Faculty of Information Science and Electrical Engineering, Kyushu University, Fukuoka 819-0395, Japan.
Email: yamamoto@ees.kyushu-u.ac.jp

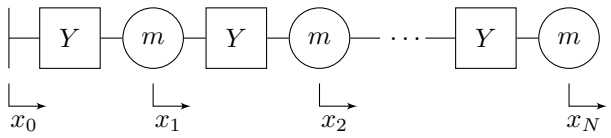


**Figure 1.** Mass chain model consisting of $N$ identical masses $m$. Each mass is connected by mechanical admittance $Y(s)$ (impedance $Z(s) = Y(s)^{-1}$).

balance between the disturbance suppression performance and the computational complexity is reasonable. It is indeed possible to extend the proposed method to higher degree admittances. However, we note that the optimisation part should be carefully treated due to the increase of the number of variables and the highly non-convex cost function.

We may note that, using the terminology introduced in the literature,[23] the graphical method in our previous paper[16] is considered as a *structure-based* approach whereas the proposed method in this paper may be classified as a *structure-immittance* approach, in the sense that an optimal topology is searched over a full set of network topologies with a fixed degree of the impedance function while it is possible to set constraints on the structural parameters.

Some background on passive mechanical networks and classical network synthesis is summarised in the next section. The problem formulation and some numerical examples will follow to illustrate the proposed method.

### General Notation

$\mathbb{C}$ and $\mathbb{Z}_+$ denote the set of complex numbers and positive integers, respectively. $\mathbb{C}_+$ is the closed right-half plane. $\mathbb{R}^{m\times n}$ is the set of $m$ by $n$ real matrices. $H^\infty$ is the standard Hardy space on the right-half plane and $\|\cdot\|_\infty$ represents the $H^\infty$-norm. In particular, the $H^\infty$-norm of a stable scaler transfer function $G(s)$ is the supremum magnitude of the frequency response $G(j\omega)$, i.e.,

$$\|G(s)\|_\infty = \sup_{\omega\in\mathbb{R}} |G(j\omega)|\,.$$

## Background on Passive Mechanical Networks

A mechanical one-port network with force-velocity pair $(F, v)$ is *passive* if for all square integrable pairs $F(t)$ and $v(t)$ on $(-\infty, T]$, $\int_{-\infty}^{T} F(t)v(t)dt \geq 0$.[24] Furthermore, a passive network is *lossless* if it satisfies the condition

$$\int_{-\infty}^{T} F(t)v(t)dt = 0.$$

For a linear time-invariant network the admittance $Y(s)$ is defined by the ratio $\hat{F}(s)/\hat{v}(s)$ where $\hat{}$ denotes the Laplace transform, and $Z(s) = Y(s)^{-1}$ is called the impedance. Such a network can be shown to be passive if and only if $Y(s)$ or $Z(s)$ is positive real.[25,26]

### Network Synthesis

The present paper considers three essential passive components: springs, dampers and *inerters*. The inerter is a mechanical two-terminal device with the property that the applied force at the terminals is proportional to the relative acceleration between the terminals. Since any real-rational positive-real function can be realised as the admittance or impedance of a network with springs, inerters, and dampers only[5], once we obtain a positive real admittance $Y(s)$ that gives a good disturbance suppression performance in a scale-free manner, the resulting admittance can be realised only by these three passive mechanical components.

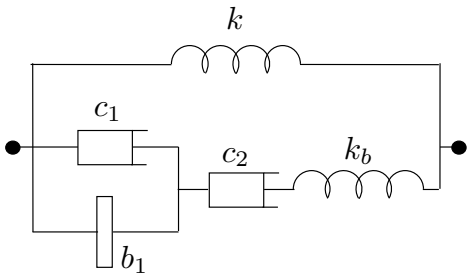


**(a)** First realisation of the admittance (1).

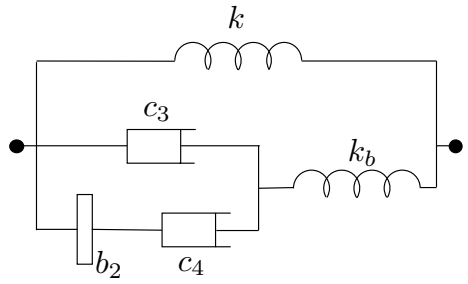


**(b)** Second realisation of the admittance (1).

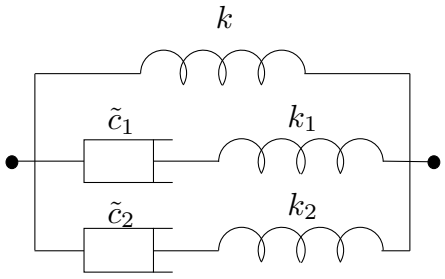


**(c)** Spring-damper realisation of the admittance (1).

**Figure 2.** Realisations of the admittance (1).

### Low Degree Positive Real Admittances

In this section, we briefly discuss the class of *arbitrary* degree-3 positive real mechanical admittances and its realisations. See the reference[5] for the detailed discussion.

Consider the real-rational function

$$Y(s) = k\frac{\alpha_0 s^2 + \alpha_1 s + 1}{s(\beta_0 s^2 + \beta_1 s + 1)} \tag{1}$$

where $\beta_0, \beta_1 \geq 0$ and $k > 0$. Then, $Y(s)$ is positive real if and only if the following three inequalities hold[5]:

$$a_1 := \alpha_0\beta_1 - \alpha_1\beta_0 \geq 0 \tag{2}$$
$$a_2 := \alpha_0 - \beta_0 \geq 0 \tag{3}$$
$$a_3 := \alpha_1 - \beta_1 \geq 0. \tag{4}$$

Define also $a_4 := a_2^2 - a_1 a_3$. If $a_2 > 0$ and $a_4 > 0$, then the realisation of the admittance (1) can be obtained by the Brune

procedure.[25] The resulting realisations are shown in Figs. 2a and 2b where

$$k_b = \frac{ka_2}{\beta_0}$$
$$c_1 = \frac{ka_2^2 a_3}{a_4} \quad c_2 = \frac{ka_2^2}{a_1} \quad b_1 = \frac{ka_2^3}{a_4}$$
$$c_3 = ka_3 \quad c_4 = \frac{ka_4}{a_1} \quad b_2 = \frac{ka_4}{a_2}.$$

It has been pointed out[5] that a straightforward computation gives $c_3 \le c_1, c_4 \le c_2$ and $b_2 \le b_1$, so the realisation of Fig. 2b is the more efficient one.

Otherwise (if either $a_2 = 0$ or $a_4 \le 0$) the realisation is given in the form of Fig. 2c. Note that if $\alpha_0 = 0$, $\beta_0 = 0$ and $a_3 > 0$, $Y(s)$ is realised with using springs and one damper.

## Problem Formulation

### *Intermass displacements in a mass chain*

We consider the mass chain of Fig. 1, where $N$ point masses $m$ are connected by identical passive mechanical admittances $Y(s)$. We assume that the interconnection consists of at least one spring in parallel with some passive components, i.e.,

$$Y(s) = k/s + Y_1(s) \tag{5}$$

where $k > 0$ and $Y_1(s)$ is a positive real admittance.

The mass chain is excited at one end, the displacement of which is denoted by $x_0(t)$. The displacement of the $i$th mass is denoted by $x_i(t)$, $i = 1, 2, \ldots, N$. The initial conditions of these displacements are assumed to be all zero. The equations of motion are then written in the Laplace transformed domain as

$$\hat{\mathbf{x}} = (h(s)\mathbf{I} - \mathbf{L}_N)^{-1}\boldsymbol{\phi}_1 \hat{x}_0 \tag{6}$$

where $\mathbf{I}$ is the identity matrix and

$$h(s) = sZ(s)m, \quad Z(s) = Y(s)^{-1},$$
$$\hat{\mathbf{x}} = [\hat{x}_1, \ldots, \hat{x}_N]^{\mathrm{T}} \in \mathbb{R}^N,$$
$$\boldsymbol{\phi}_1 = [1,\ 0, \ldots,\ 0]^{\mathrm{T}} \in \mathbb{R}^N,$$
$$\mathbf{L}_N = \begin{bmatrix} -2 & 1 & 0 & \cdots & 0 \\ 1 & -2 & 1 & \ddots & \vdots \\ 0 & \ddots & \ddots & \ddots & 0 \\ \vdots & \ddots & 1 & -2 & 1 \\ 0 & \cdots & 0 & 1 & -1 \end{bmatrix} \in \mathbb{R}^{N\times N}.$$

The characteristic polynomials $d_i$ of $\mathbf{L}_i \in \mathbb{R}^{i\times i}$ in the variable $h$ is given by

$$d_i = \det(h\mathbf{I} - \mathbf{L}_i). \tag{7}$$

We find that

$$d_i(h) = (h+2)d_{i-1}(h) - d_{i-2}(h) \quad \text{for } i = 1, \ldots, N \tag{8}$$

where $d_{-1} = 1$ and $d_0 = 1$. Using $d_i$, eq. (6) is written as

$$\hat{\mathbf{x}} = \frac{\mathrm{adj}(h(s)\mathbf{I} - \mathbf{L}_N)}{\det(h(s)\mathbf{I} - \mathbf{L}_N)}\boldsymbol{\phi}_1 \hat{x}_0 = \frac{1}{d_N}\begin{pmatrix} d_{N-1} \\ \vdots \\ d_0 \end{pmatrix} \hat{x}_0. \tag{9}$$

Let $F_N^{(i)}(h(s))$ denote the transfer function from $x_0$ to a given intermass displacement, $x_{i-1} - x_i$, $i = 1, 2, \ldots, N$. The subscript $N$ specifies the total number of masses in the chain. Hence, for $i = 1, 2, \ldots, N$,

$$F_N^{(i)}(h(s)) = \frac{d_{N-i+1} - d_{N-i}}{d_N}. \tag{10}$$

Treating $h$ as the independent variable, it is straightforward to see that the roots of $d_i(h)$ lie in the interval $(-4, 0)$ by using the Gershgorin's disc bound on the eigenvalues of Hermitian matrix $\mathbf{L}_N$ (guaranteeing the roots lie in the closed interval $[-4, 0]$) and by directly checking that $d_i(0)$ and $d_i(-4)$ are nonzero for all $i \in \mathbb{Z}_+$. (The interested reader is referred to the proof of Theorem 1 in the reference.[16]) The system of Fig. 1 is stable if $d_N(h(s)) \neq 0$ for any $s \in \mathbb{C}_+$. For $0 \not\equiv Y(s)$ positive real, it is sufficient to guarantee the stability if $h(s)$ does not take values in the interval $(-4, 0)$ for any $s$ with $\mathrm{Re}(s) = 0$. This is equivalent to the condition that $h(j\omega)$ does not touch the imaginary axis between $(0, j4)$, which is a very mild condition that is hard to violate in practice. Under this condition, it has been previously proved[16,19] that the $H^\infty$-norm of the transfer function $F_N^{(i)}(h(s))$ is uniformly bounded with respect to $N$ with the following additional sufficient condition:

$$Y_1(0) > 0,$$

where $Y_1(s)$ is as defined in eq. (5).

In the sequel, we focus on the interconnection design that suppresses the $H^\infty$-norm of $F_N^{(i)}(h(s))$ well for an arbitrary length of the mass chain. A (sub)optimal solution of such an interconnection admittance $Y(s)$ is searched over the class of arbitrary degree-3 positive real mechanical admittances (1). We now consider the following constrained optimisation problem:

**Problem 1.**

$$\begin{aligned} \text{Minimize} \quad & \gamma(\alpha_0, \alpha_1, \beta_0, \beta_1) \\ \text{subject to} \quad & \|W(s)F_N^{(i)}(h(s))\|_\infty \le \gamma(\alpha_0, \alpha_1, \beta_0, \beta_1) \\ & \qquad \forall N, i \in \mathbb{Z}_+, \\ & h(s) = \frac{ms^2(\beta_0 s^2 + \beta_1 s + 1)}{k(\alpha_0 s^2 + \alpha_1 s + 1)}, \\ & \beta_0, \beta_1 \ge 0, \\ & k, m > 0, \\ & \alpha_0\beta_1 - \alpha_1\beta_0 \ge 0, \\ & \alpha_0 - \beta_0 \ge 0, \\ & \alpha_1 - \beta_1 > 0 \end{aligned} \tag{11}$$

where $W(s)$ is a weighting function.

$\gamma(\alpha_0, \alpha_1, \beta_0, \beta_1)$ is the upper bound of the $H^\infty$-norm of $W(s)F_N^{(i)}(h(s))$, the weighted transfer function from the disturbance to an $i$-th intermass displacement, over all $N \in \mathbb{Z}_+$ and $i \le N$. Note that $F_N^{(i)}(h(s))$ is in the form of (10). Using the recurrence relation (7), it is possible to efficiently compute $\|F_N^{(i)}(h(s))\|_\infty$ for various $N$.

$\alpha_0, \alpha_1, \beta_0, \beta_1$ are the optimisation variables. Note that $h(s) = sY(s)^{-1}m$ where $Y(s)$ is the admittance (1). Hence, the last three inequalities are the necessary and sufficient

condition for $Y(s)$ to be positive real (2)–(4) where the final condition is replaced by a strict inequality. This is to satisfy $Y_1(0) > 0$, which is one of the sufficient conditions to achieve uniform boundedness.[16,19] Indeed, since

$$Y(s) = k\frac{\alpha_0 s^2 + \alpha_1 s + 1}{s(\beta_0 s^2 + \beta_1 s + 1)} = \frac{k}{s} + \underbrace{\frac{k(\alpha_0 - \beta_0)s + \alpha_1 - \beta_1}{\beta_0 s^2 + \beta_1 s + 1}}_{Y_1(s)},$$

the inequality $\alpha_1 - \beta_1 > 0$ implies $Y_1(0) > 0$.

To solve this problem numerically, we need to search over finite $N$, i.e., $1 \le N \le N_0$. We may note that this will not affect the optimisation result as long as we choose a large enough $N_0$ in practice, based on the observation in the reference[16] that $F_N^{(i)}(h(s))$ for each $s \in \mathbb{C}$ converges quickly to its fixed point when we select the interconnection $h(s)$ such that $\|F_N^{(i)}(h(s))\|_\infty \le 1$.

Once this problem is solved, the optimal configuration is realised following the procedure stated in the previous section *"Low Degree Positive Real Admittances."*

### *Effect of $\beta_0$*

We first investigate how the parameter $\beta_0$ affects the objective function $\gamma(\alpha_0, \alpha_1, \beta_0, \beta_1)$. Let us introduce a complex variable $g$ which is a reciprocal of $h$, i.e., $g(s) := h^{-1}(s) = Y(s)/(ms)$. Figure 3 shows the contour plot of $\max_{1\le N\le 200}|F_N^{(i)}(h)|$ in the $g$-plane. We see that the infinity norm takes a large value if $g$ is closer to the real axis between $(-\infty, -1/4]$. Since

$$g(s) = \frac{Y(s)}{ms} = \frac{k}{ms^2} + \frac{k(\alpha_0 - \beta_0)s + \alpha_1 - \beta_1}{ms(\beta_0 s^2 + \beta_1 s + 1)},$$

the real part and the imaginary part of $g(j\omega)$ are, respectively,

$$\mathrm{Re}(g(j\omega)) = -\frac{k}{m\omega^2} + \frac{k(a_2(1-\beta_0\omega^2) - a_3\beta_1)}{m((1-\beta_0\omega^2)^2 + \beta_1^2\omega^2)}$$
$$\mathrm{Im}(g(j\omega)) = -\frac{k(a_1\omega^2 + a_3)}{m((1-\beta_0\omega^2)^2 + \beta_1^2\omega^2)}.$$

It is observed from the denominator of the imaginary part of $g(j\omega)$ that if $\beta_0 \neq 0$ $\mathrm{Im}(g(j\omega))$ takes small values in a wide frequency range. The loci of $g(j\omega)$ with different values of $\beta_0$ are plotted on the contour plot in Fig. 4 where $\alpha_0 = 1, \alpha_1 = 1, \beta_1 = 0.1$. We see that $g(j\omega)$ becomes closer to the real axis between $(-\infty, -1/4]$ as we make $\beta_0$ larger. Hence, it is desired to set $\beta_0 = 0$ when possible. This means that $k_b = ka_2/\beta_0 = \infty$ in Fig. 2a and Fig. 2b. However, some mechanical devices cannot be assumed to be totally rigid, i.e., $k_b \neq \infty$. The effect of this is further investigated through numerical examples.

## Interconnection Design

For the numerical examples, we choose the following parameters: $m = 1.0$ kg (normalised), $k = 1700$ Nm$^{-1}$, and $N_0 = 200$ (the maximum number of $N$ to be searched over).

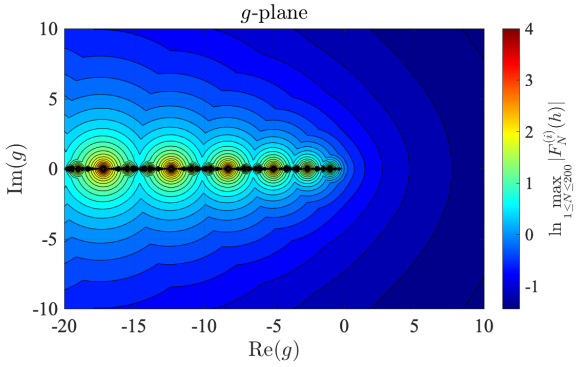


**Figure 3.** Contour plot of $\max_{1\le N\le 200}|F_N^{(i)}(h)|$ where $h = g^{-1}$.

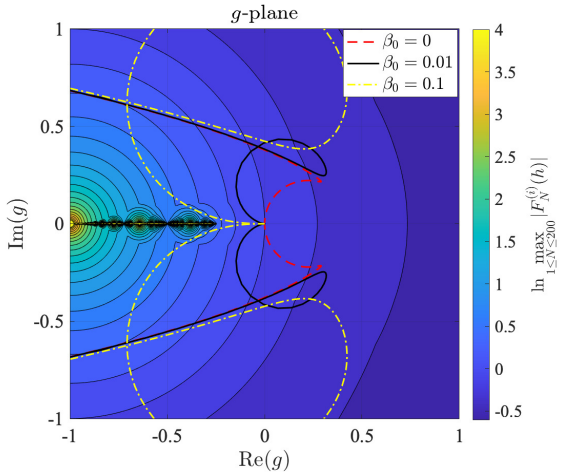


**Figure 4.** Loci of $g(j\omega)$ with different values of $\beta_0$ on the contour plot of $\max_{1\le N\le 200}|F_N^{(i)}(h)|$.

### *Optimising over all frequency range*

We first consider the case of optimising over all frequency range without introducing any frequency weight $W(s)$. Observe that

$$\gamma(\alpha_0, \alpha_1, \beta_0, \beta_1) \ge \sup_i \sup_{N\ge i} \|F_N^{(i)}(h(s))\|_\infty \ge \|F_1^{(1)}(h(s))\|_\infty$$

where

$$F_1^{(1)}(h(s)) = \frac{h(s)}{h(s)+1},$$

which is obtained from (10). If $h(s)$ takes the form (11) and either $\beta_0 \neq 0$ or $\beta_1 \neq 0$, then $|h(j\omega)| \to \infty$ as $\omega \to \infty$. Consequently, $\|F_1^{(1)}(h(s))\|_\infty$, the lower bound of $\gamma$, takes a value greater than or equal to 1. Hence, to further improve $\gamma$, we need $\beta_0 = \beta_1 = 0$, which results in the admittance of the form

$$Y(s) = \frac{k}{s} + k\alpha_1 + k\alpha_0 s, \tag{12}$$

the realisation of which is the configuration consisting of one spring $k$, one damper $c = k\alpha_1$, and one inerter $b = k\alpha_0$ in

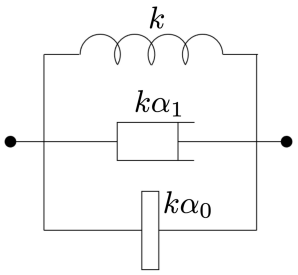


**Figure 5.** Optimal configuration when all the frequency range is considered.

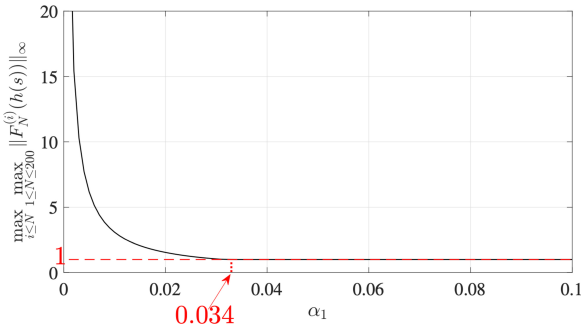


**Figure 6.** Plot of $\max_{i\le N}\max_{1\le N\le 200}\|F_N^{(i)}(h(s))\|_\infty$ versus $\alpha_1$.

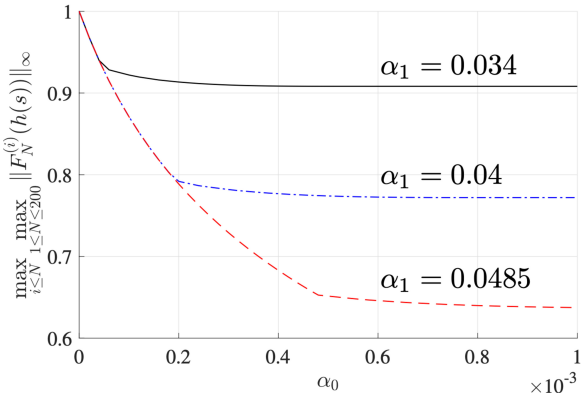


**Figure 7.** Plot of $\max_{i\le N}\max_{1\le N\le 200}\|F_N^{(i)}(h(s))\|_\infty$ versus $\alpha_0$.

parallel as shown in Fig. 5. That is,

$$k_b = \infty, \qquad c_1 = c_3 = k\alpha_1,$$
$$c_2 = c_4 = \infty, \quad b_1 = b_2 = k\alpha_0$$

in Figs. 2a and 2b. Note that the configuration consists of one spring and one damper only without an inerter, i.e., $\alpha_0 = 0$, $|F_1^{(1)}(h(j\omega))|$ again approaches 1 as $\omega \to \infty$ which results in $\gamma(\alpha_0, \alpha_1, \beta_0, \beta_1) \ge 1$ as shown in Fig. 6. It is also observed that for $\alpha_1 \ge 0.034$, the value $\max_{i\le N}\max_{1\le N\le 200}\|F_N^{(i)}(h(s))\|_\infty$ stays 1. Adding an inerter in parallel improves the performance as shown in Fig. 7. It is also worth noting that the rate of decrease in the objective function slows down at a certain value of $\alpha_0$ and this value seems to have a correlation with $\alpha_1$. We remark that the mass chain with $N = 1$ and the interconnection admittance in (12) with $(\alpha_0, \alpha_1) = (0, 0.0485)$ corresponds to a critically damped harmonic oscillator, the damping ratio of which is $\zeta = k\alpha_1/(2\sqrt{mk}) = 1$.

### *Optimising over a certain frequency range with constraints on structural parameters*

In this subsection, we consider setting constraints on structural parameters. We first set $\beta_0 = 0$ corresponding to $k_b = \infty$. Based on the observation in Section 2 that the realisation of Fig. 2b is more efficient than that of Fig. 2a, we derive the conditions on $\alpha_0, \alpha_1, \beta_0, \beta_1$ to set the upper bounds $\bar{b}_2, \bar{c}_3, \bar{c}_4$ on $b_2, c_3, c_4$ in Fig. 2b. Since

$$c_3 = ka_3, \quad c_4 = \frac{ka_4}{a_1}, \quad b_2 = \frac{ka_4}{a_2},$$

noting $\beta_0 = 0$, we have the following additional nonlinear constraints on $\alpha_0, \alpha_1, \beta_0, \beta_1$ to Problem 1:

$$a_3 = \alpha_1 - \beta_1 \le \frac{\bar{c}_3}{k},$$
$$\frac{a_4}{a_1} = \frac{\alpha_0}{\beta_1} - (\alpha_1 - \beta_1) \le \frac{\bar{c}_4}{k},$$
$$\frac{a_4}{a_2} = \alpha_0 - \beta_1(\alpha_1 - \beta_1) \le \frac{\bar{b}_2}{k}.$$

In the following example, we set

$$\frac{\bar{c}_3}{k} = 0.04, \quad \frac{\bar{b}_2}{k} = 5 \times 10^{-4}$$

without setting a constraint on the damping coefficient $c_4$, leaving the possibility of $c_4 = \infty$ open.

We now introduce the weight

$$W(s) = \frac{1}{0.05s + 1} \tag{13}$$

and solve Problem 1 with the above constraints on structural parameters. MATLAB's nonlinear programming solver `fmincon` led to the following parameters :

$$\alpha_0 = 0.1250, \quad \alpha_1 = 3.1522, \quad \beta_0 = 0, \quad \beta_1 = 3.1122.$$

The values for the constants in the realisations of Fig. 2b are given by (after rounding small numbers) $k_b = \infty$ and

$$c_3 = 68.00\ \text{Nsm}^{-1},\ c_4 = 0.2720\ \text{Nsm}^{-1},\ b_2 = 0.8466\ \text{kg} \tag{14}$$

as illustrated in Fig. 8. The frequency domain plot of $\max_i |W(j\omega)F_N^{(i)}(h(j\omega))|$ in Fig. 9 shows that the weighted frequency response is well suppressed for various length of mass chains. The time responses of the first intermass displacements of these mass chains are also shown in Fig. 10 where the input is the recorded earthquake ground motion of JMA Kobe NS 1995.[27] We note that, in all the cases, the first intermass displacements exhibited the maximum amplitude over time among all the intermass displacements. The time response of the uncontrolled mass chain of length 10 ($N = 10$) is also shown for comparison. Here 'uncontrolled' means that the masses are connected by a spring $k$ with 2 % of structural damping. We may see that, comparing to the uncontrolled case, the optimal configuration suppresses the intermass displacements effectively with better transient response. We may however note that our problem setting of minimising the $H^\infty$-norm cannot directly consider the transient response in general. For example, the slow decay rate in a vehicle platooning reported in the reference[28] may still persist.

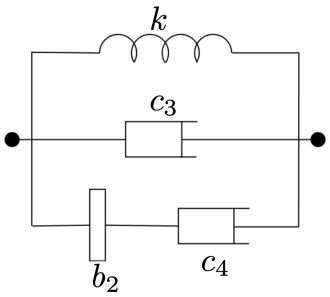


**Figure 8.** Optimal configuration when a frequency weighting and some constraints on structural parameters are introduced. The parameters are given in (14).

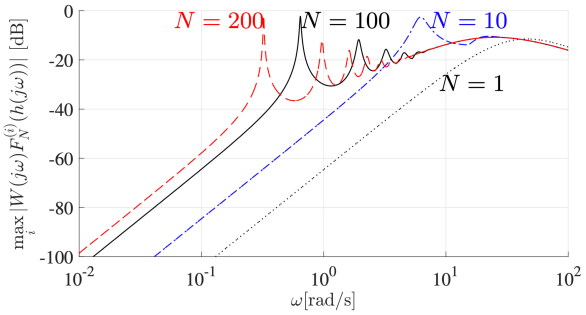


**Figure 9.** $\max_i |W(j\omega)F_N^{(i)}(h(j\omega))|$ with the structural parameters (14) and $k_b = \infty$ for $N = 1, 10, 100, 200$.

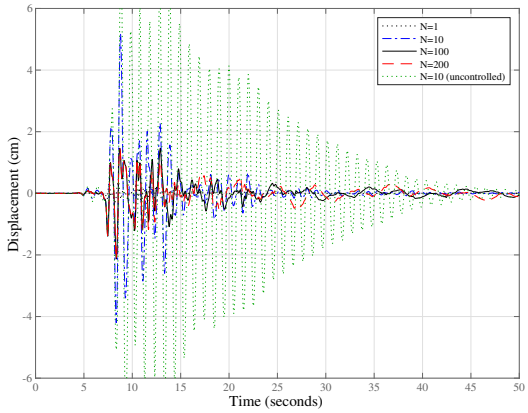


**Figure 10.** Time responses of the first intermass displacement of various length of mass chains subjected to JMA Kobe NS earthquake. The structural parameters are given in (14).

## *Effect of $k_b$*

In the previous two examples the optimal configurations required $\beta_0 = 0$, which gives $k_b = \infty$. However, some mechanical devices cannot be assumed to be totally rigid, i.e., $k_b \neq \infty$. In this example, we investigate how this affects an optimal configuration. For $k_b \neq \infty$, $\beta_0$ must be strictly positive. Since $k_b = ka_2/\beta_0 = k(\alpha_0/\beta_0 - 1)$, Problem 1 can be restated as

$$
\begin{aligned}
\text{Minimize} \quad & \gamma(\alpha_1, \beta_0, \beta_1), \\
\text{subject to} \quad & \|W(s)F_N^{(i)}(h(s))\|_\infty \leq \gamma(\alpha_1, \beta_0, \beta_1) \\
& \qquad \forall N, i \in \mathbb{Z}_+, \\
& h(s) = \frac{ms^2(\beta_0 s^2 + \beta_1 s + 1)}{k\left(\left(1 + \frac{k_b}{k}\right)\beta_0 s^2 + \alpha_1 s + 1\right)}, \\
& \beta_0 > 0, \quad \beta_1 \geq 0, \\
& k, m > 0, \\
& \left(1 + \frac{k_b}{k}\right)\beta_1 - \alpha_1 \geq 0, \\
& \alpha_1 - \beta_1 > 0.
\end{aligned}
$$

We set $k_b/k = 0.5$ and employ the same weighting function of (13).

MATLAB's `fmincon` led to the following parameters:

$$
\alpha_0 = 4.915 \times 10^{-4}, \quad \alpha_1 = 4.962 \times 10^{-2},
$$
$$
\beta_0 = 3.277 \times 10^{-4}, \quad \beta_1 = 3.308 \times 10^{-2}.
$$

where $\alpha_0$ was computed by $\alpha_0 = \beta_0(1 + k_b/k)$. The values for the constants in the realisations of Fig. 2a and Fig. 2b are given by $k_b = 850\ \text{Nm}^{-1}$ and

$$
\begin{aligned}
& c_1 = c_3 = 28.12\ \text{Nsm}^{-1}, \quad c_2 = c_4 = \infty, \\
& b_1 = b_2 = 0.2785\ \text{kg}, \qquad (15)
\end{aligned}
$$

i.e., one spring, one damper, and one inerter in parallel as shown in Fig. 11. It is interesting that a larger damping does not improve the vibration suppression performance in this case. The value of $\max_{i \leq N} \max_{1 \leq N \leq 200} \|W(s)F_N^{(i)}(h(s))\|_\infty$ is 1.867 for the optimal configuration (15), whereas it is 4.471 when the damping coefficient $c_1$ (or $c_3$) is replaced to $68.00\text{Nsm}^{-1}$. The frequency domain plot of $\max_i |W(j\omega)F_N^{(i)}(h(j\omega))|$ of the optimal configuration (15) in this example is shown in Fig. 12. As a comparison, the frequency domain plot of $\max_i |W(j\omega)F_N^{(i)}(h(j\omega))|$ of the optimal configuration (14) for $k_b = \infty$ in the previous example in Section 4 is given in Fig. 13. Note that here we set $k_b = 0.5k = 850\text{Nm}^{-1}$, not $k_b = \infty$. We see that for $N = 1$ the peak value of the frequency response is reduced significantly by using the optimal configuration (15). However, it is worth noting that for longer mass chains such as $N = 10, 100, 200$, the peak values are suppressed better when using the configuration (14). We may note that, if we rather focus on improving the disturbance suppression performance for these $N$'s, it is also possible to tune the range of $N$ in the optimisation problem 1. That is, we may try to minimise the objective function for $10 \leq N \leq 200$ instead of $1 \leq N \leq 200$ for example.

**Remark 1.** *Due to its nonconvexity, achieving global minima in Problem 1 cannot be guaranteed in general. The numerical solutions given in this paper, i.e., the configurations (14) and (15), are only guaranteed to be a local minimum.*

**Remark 2.** *The default setting (an interior-point method) of `fmincon` was used for the numerical simulations in this paper.*

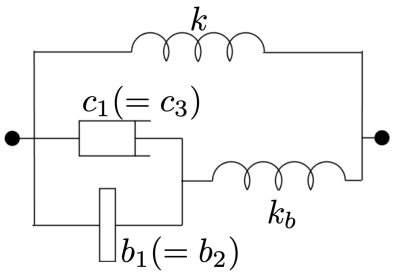


**Figure 11.** Optimal configuration when the effect of $k_b$ is considered. The parameters are given in (15).

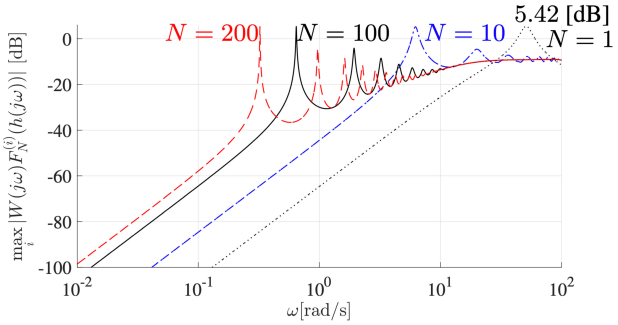


**Figure 12.** $\max_i |W(j\omega)F_N^{(i)}(h(j\omega))|$ with the structural parameters (15) and $k_b = 0.5k$ for $N = 1, 10, 100, 200$.

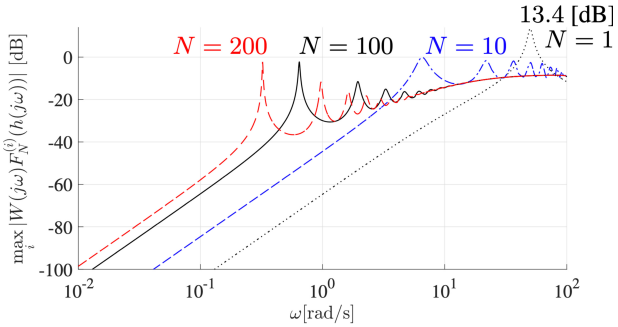


**Figure 13.** $\max_i |W(j\omega)F_N^{(i)}(h(j\omega))|$ with the structural parameters (14) and $k_b = 0.5k$ for $N = 1, 10, 100, 200$.

## Conclusions

The synthesis problem of the passive interconnection in a homogeneous mass chain has been studied. The chain is excited at one end and the interconnection admittance is designed to suppress the disturbance independent of the length of the mass chain. An optimisation problem has been proposed to achieve a scale-free disturbance suppression performance. A suitable choice of such admittance has been searched over a class of arbitrary positive real function of a fixed (low) degree, which has the realisations consisting of springs, at most two dampers, and one inerter. Although the problem formulation can be extended to higher degree cases, the selection of a more suitable optimisation algorithm is required and considered as future work.

### Acknowledgements

This work has been supported in part by the Japan Society for the Promotion of Science under Grants-in-Aid for Scientific Research No. 20K14766.and No. 19H02161.

### References

1. Fujita K, Yamamoto K and Takewaki I. An evolutionary algorithm for optimal damper placement to minimize interstorey-drift transfer function in shear building. *Earthquakes and Structures* 2010; 1(3): 289–306.
2. Lazar I, Neild S and Wagg D. Using an inerter-based device for structural vibration suppression. *Earthquake Engineering & Structural Dynamics* 2014; 43(8): 1129–1147.
3. Jalili N and Olgac N. Multiple delayed resonator vibration absorbers for multi-degree-of-freedom mechanical structures. *Journal of Sound and Vibration* 1999; 223(4): 567–585.
4. Hu Y and Chen MZ. Performance evaluation for inerter-based dynamic vibration absorbers. *International Journal of Mechanical Sciences* 2015; 99: 297–307.
5. Smith MC. Synthesis of mechanical networks: The inerter. *IEEE Transactions on Automatic Control* 2002; 47(10): 1648–1662.
6. Takewaki I, Murakami S, Yoshitomi S et al. Fundamental mechanism of earthquake response reduction in building structures with inertial dampers. *Structural Control and Health Monitoring* 2012; 19(6): 590–608.
7. Giaralis A and Petrini F. Optimum design of the tuned mass-damper-inerter for serviceability limit state performance in wind-excited tall buildings. *Procedia engineering* 2017; 199: 1773–1778.
8. Chen MZQ and Hu Y. *Inerter and Its Application in Vibration Control Systems*. Springer Singapore, 2019.
9. Chen MZ, Hu Y, Huang L et al. Influence of inerter on natural frequencies of vibration systems. *Journal of Sound and Vibration* 2014; 333(7): 1874–1887.
10. Hu Y, Chen MZ and Smith MC. Natural frequency assignment for mass-chain systems with inerters. *Mechanical Systems and Signal Processing* 2018; 108: 126–139.
11. Seiler P, Pant A and Hedrick K. Disturbance propagation in vehicle strings. *IEEE Transactions on Automatic Control* 2004; 49(10): 1835–1842.
12. Barooah P and Hespanha J. Error amplification and disturbance propagation in vehicle strings with decentralized linear control. In *44th IEEE Conference on Decision and Control and European Control Conference*. pp. 4964–4969.
13. Farnam A and Crevecoeur G. Guaranteeing string stability of multiple interconnected vehicles using heterogeneous controllers. *Journal of Dynamic Systems, Measurement, and Control* 2020; .
14. Bamieh B, Jovanovic M, Mitra P et al. Coherence in large-scale networks: Dimension-dependent limitations of local feedback. *IEEE Transactions on Automatic Control* 2012; 57(9): 2235–2249.
15. Pates R. A loopshaping approach to controller design in networks of linear systems. In *54th IEEE Conference on Decision and Control*. pp. 6276–6281.
16. Yamamoto K and Smith MC. Bounded disturbance amplification for mass chains with passive interconnection. *IEEE Transactions on Automatic Control* 2016; 61(6): 1565–1574.
17. Farnam A and Sarlette A. String stability towards leader thanks to asymmetric bidirectional controller. *IFAC-PapersOnLine* 2017; 50(1): 10335 – 10341. 20th IFAC World Congress.
18. Pates R and Yamamoto K. Scale free bounds on the amplification of disturbances in mass chains. In *2018 Annual*

*American Control Conference (ACC)*. pp. 6002–6005.
19. Yamamoto K. *Disturbance Attenuation in Mass Chains with Passive Interconnection*. PhD Thesis, University of Cambridge, 2016.
20. Yamamoto K and Smith MC. Mass chains with passive interconnection: Complex iterative maps and scalability. In *52nd IEEE Conference on Decision and Control*. pp. 37–42.
21. Yamamoto K and Smith MC. Design of passive interconnections in tall buildings subject to earthquake disturbances to suppress inter-storey drifts. *Journal of Physics: Conference Series* 2016; 744: 012063.
22. Chen MZ, Papageorgiou C, Scheibe F et al. The missing mechanical circuit element. *IEEE Circuits and Systems Magazine* 2009; 9(1): 10–26.
23. Zhang SY, Jiang JZ and Neild SA. Passive vibration control: a structure–immittance approach. *Proceedings of the Royal Society A: Mathematical, Physical and Engineering Sciences* 2017; 473(2201): 20170011.
24. Anderson BDO and Vongpanitlerd S. *Network Analysis and Synthesis: A Modern Systems Theory Approach (Dover Books on Engineering)*. Dover Publications, 2006.
25. Brune O. Synthesis of a finite two-terminal network whose driving-point impedance is a prescribed function of frequency. *J Math Phys* 1931; 10: 191–236.
26. Valkenburg MEV. *Introduction to Modern Network Synthesis*. Wiley, 1960.
27. Iwasaki Y and Tai M. Strong motion records at kobe port island. *Soils and foundations* 1996; 36(Special): 29–40.
28. Jovanovic M and Bamieh B. On the ill-posedness of certain vehicular platoon control problems. *IEEE Trans Automat Contr* 2005; 50(9): 1307–1321.